Tip-Tilt-Piston Micromirror with Integrated Large Range Variable Focus for Smart Lighting Systems

J. Morrison,[1] M. Imboden,[2] T. D. C. Little,[2] D. J. Bishop[1,2,3]
[1]*Department of Physics, Boston University, Boston, Massachusetts, USA, morrisja@bu.edu*
[2]*Department of Electrical and Computer Engineering, Boston University, Boston, Massachusetts, USA*
[3]*Division of Materials Science and Engineering, Boston University, Brookline, Massachusetts, USA*

ABSTRACT

We demonstrate a novel MOEMS mirror which integrates variable focus and dynamic beam steering, eliminating the need for multiple microsystems. The mirror provides ±40° optical deflection and a variable focal length which can be tuned from -0.48 mm to +20.5 mm. The mirror also can be actuated in a piston mode over a 168 μm range. The dynamics of the mirror are studied and a methodology for tuning the resonant frequencies is explored. The large optical deflection and variable focus ranges provide unique advantages in Smart Lighting systems, where field of view and dynamic optics are growing in demand due to the high mobility of handheld receivers within the lighting field.

Keywords: frequency tuning, optical MEMS, electrothermal actuation.

1 INTRODUCTION

Modern fabrication techniques are enabling the adoption of micro-opto-electromechanical systems devices in applications never before anticipated. Low-cost lighting systems can exploit micromirrors to both enable directed or sculpted light and to support short-range optical communications. The latter application is intended to use visible light as an alternative to the RF spectrum to gain new wireless data capacity under diminishing RF availability. However, optical communication systems are typically limited by line-of-sight obstructions and, in LED-based Smart Lighting systems, low signal to noise ratios (SNR). While SNR can be improved by introducing beamforming techniques, the line-of-sight issue requires multiple access points with integrated beam steering.

This paper presents a dynamic study of the multi-degree of freedom micromirror discussed in reference [1] with large deflections and variable focus. The rotational symmetry and identical spring systems provide simple mapping from actuation power to angular deflection. However, these two properties induce degenerate resonance modes for tip and tilt scanning. Much has been done to mode-match vibratory MEMS such as gyroscopes [2]. In contrast, a system where degeneracies are suppressed is desireable in many applications such as in large deflection systems. For instance, the use of a scanning mode for color control in standard illumination and projection systems is a use case scenario where decoupled resonance modes are desired. We discuss utilizing induced mechanical stresses in a serpentine spring and bimorph system to decouple degenerate resonant modes to increase the range of one mode and decrease the energy lost to the degenerate mode is discussed.

2 MIRROR DESIGN

The micromirror is fabricated by MEMSCAP using the PolyMUMPS process [3]. In this process, there is one immobile polysilicon layer, two layers of polysilicon which can be used as active mechanical layers and a gold layer atop the uppermost polysilicon layer. The design presented in this paper uses the residual stresses in the gold and top-most polysilicon layer as a thermomechanical bimorph actuator in both the beam steering and dynamic focus degrees of freedom. In both cases, a combination of Joule heating and the difference in coefficients of thermal expansion allow for large deflections of the steering "legs" and the variable focus "wedges".

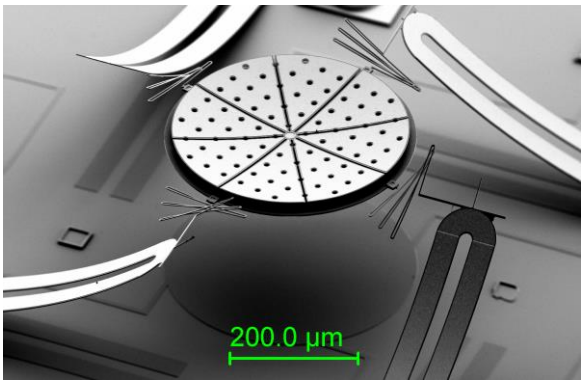

Figure 1: SEM image of large range tip-tilt-piston micromirror with integrated variable focus.

A voltage bias across the bimorph legs results in power dissipation throughout the actuated leg. The thermal stresses induce a bending moment along the bimorph leg resulting in a large vertical tip displacement. The four serpentine springs extending out from the mirror are vital to both the mechanical and the thermal properties of the mirror. While the springs allow for an initial projection of the mirror out of the plane upon release and provide the flexure needed for large deflections of the mirror, they also act as heat sources for the mirror bimorph wedges. A large

impedence mismatch between the bimorph legs and the polysilicon serpentine springs allows for full and independent control of angular deflection, piston mode and tunable focus. A full description of a similar devices can be found in reference [1].

3 STATIC DEFLECTIONS

Previous designs incorporated 1000 μm long bimorph legs in an effort to improve angular deflection. The length of the bimorph legs largely governs the amount of lateral motion of the tip of the bimorph demonstrated in Fig. 2(a) and 2(b). While providing the required height, the added length decreases efficiency as the first few milliwatts of power contribute only to lateral motion. Additionally, gold on polysilicon bimorphs become unstable as a threshold temperature is reached [4], narrowing the window in which a vertical displacement can be obtained for long beams. By reducing the length of the bimorph legs from 1000 μm to 600 μm, the lateral displacement is greatly reduced and the angular displacement of the mirror is more easily obtained. Short bimorphs also improve linearity in the tip/tilt angle versus dissipated electrical power in the bimorph legs. Fig. 2(c) and 2(d) demonstrate the dynamic range of the focal length. The geometry and actuation of the focal length are exactly the same as has been demonstrated in previous work [1].

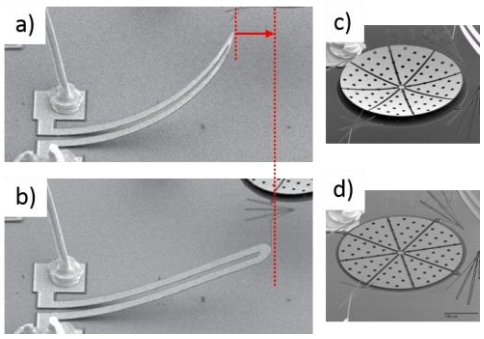

Figure 2: SEM images showing a bimorph leg (a) unactuated and (b) actuated and the variable focus mirror (c) unactuated and (d) actuated.

Prior to the angular measurements a current-voltage sweep was conducted. The power-voltage relationship was then used to form an open-loop driven system using a voltage look-up table. For each static angular measurement, the mirror was voltage biased and the current and voltage were recorded using a four-point probe.

3.1 Angular Range

The angular deflections for varying drive techniques were tested for both devices and are shown in Fig. 3. The diagonal range is measured using a power differential actuation where the four bimorphs are actuated at 12 mW to begin. From point of symmetry (12 mW), two adjacent bimorphs are increased while the other two are decreased until the power is 24 mW (or 0 mW). A greater error in power is associated with the differential measurements because the deflection associated with a 4 mW power differential symmetric about 10 mW does not produce the same deflection for one symmetric about 12 mW.

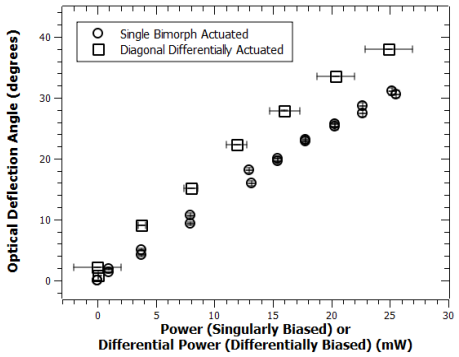

Figure 3: The optical deflection for diagonal differential actuation (square), singular actuation (circle). Some error bars are too small to be seen.

3.2 Vertical Range

The vertical range of the mirror was measured using a Zygo optical interferometer. The bimorph legs were attached in series and current biased to ensure the same power dissipation in all four bimorph legs. Fig. 4 shows the vertical deflection as a function of the total power dissipated.

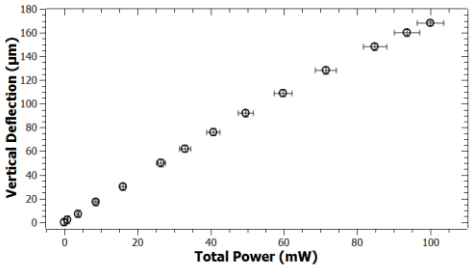

Figure 4: The vertical deflection of the micromirror is shown as a function of total power dissipated.

4 DYNAMICS

4.1 Resonant Modes

Frequency scans were obtained when applying a differential AC voltage bias shown in Fig. 5 on two legs, while the other two legs were biased with $V_{offset,a(b)}$. The deflections were measured using a 2D position sensitive detector (PSD). The output of the PSD was coupled to a lock-in amplifier and recorded during each frequency sweep. Using the output from the PSD and the measured position of the PSD relative to the mirror, the magnitude of

the angle was extrapolated and recorded during each frequency sweep.

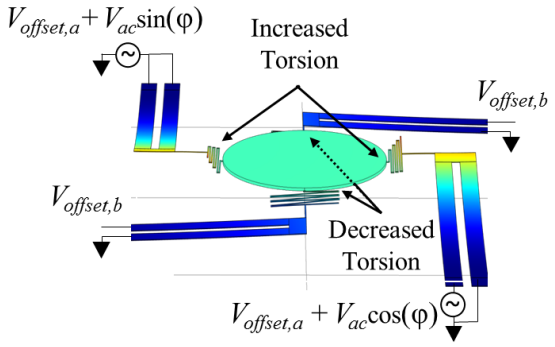

Figure 5: FEM simulations of the mirror showing the difference in mechanical strain in the serpentine springs connected to bimorph legs with a nonzero offset power $V_{offset,b}$ with an overlay of the differential driving circuit.

Finite element method (FEM) simulations of the device were conducted using COMSOL Multiphysics. The simulation eigenfrequencies of the mirror system were 1065 Hz for the piston mode and 1762 Hz for the degenerate tip and tilt modes. The measured resonances with zero offset and a V_{ac} peak-to-peak value of 3 mV are 1552 Hz for both tip and tilt modes depicted in Fig. 6. The offset voltage for the frequency response shown in Fig. 6 is $V_{offset,a(b)}$ = 0 mV. The piston mode resonance position is located at 500 Hz with a higher order piston mode located at 1 kHz. The simulations did not include the release holes and slight variations in the gold/polysilicon ratio due to design rules for PolyMUMPS.

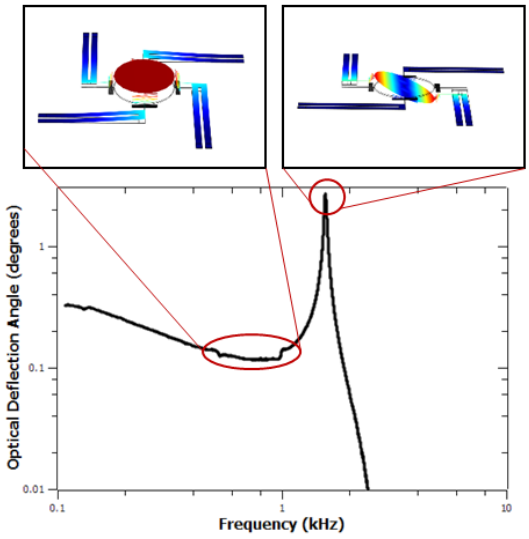

Figure 6: The measured frequency response data with zero offset voltages is provided showing the corresponding mode shapes as simulated in COMSOL.

4.2 Mechanical Stress Induced Resonant Mode Decoupling

Perfectly matched modes are useful for circular scanning but need to be suppressed for raster scanning. In the context of illumination and directional lighting, the most useful scenario is a large angle raster scan. To provide this capability, a method was constructed to either suppress the unwanted mode or to separate the modes while maintaining large amplitudes. The principle behind the decoupling is dynamically changing the strain in the serpentine springs and bimorph legs. As shown in Fig. 7, actuation of a bimorph leg drastically alters the torsional and bending strain in the corresponding serpentine spring. Simultaneous actuation of opposite bimorph legs reduces the effective spring constant of the mode associated with rotation of the affected springs. In addition, the effective spring constant of the mode associated with rotation about the unactuated serpentine springs is increased slightly. Fig. 5 shows the simulated deformation of the serpentine springs upon applying a nonzero $V_{offset,b}$ while holding $V_{offset,a}$ = 0 mV.

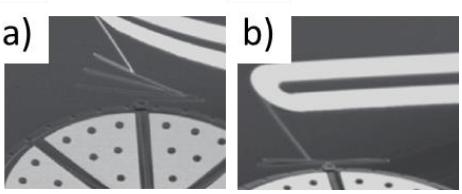

Figure 7: SEM images showing the spring deformation (a) prior to acuation and (b) during actuation of the bimorph.

Similar methodologies have been proven effective in scanning micromirrors for shifting a single mode by using a separate actuator [5], [6].

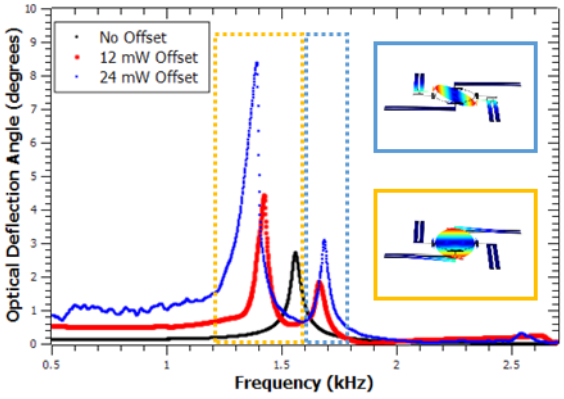

Figure 8: Measured frequency response data for varying $V_{offset,a}$ for a power of 0 mW, 12 mW and 24 mW in each of the offset bimorphs. Insets are mode shapes simulated in COMSOL.

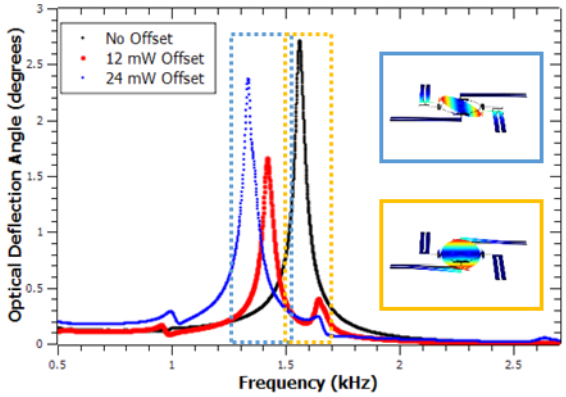

Figure 9: Measured frequency response data for varying $V_{offset,b}$ for a power of 0 mW, 12 mW and 24 mW in each of the offset bimorphs. Insets are simulated mode shapes.

The frequency response for variations in $V_{offset,a}$ and $V_{offset,b}$ corresponding to dissipated power in each of the offset bimorphs are shown in Fig. 8 and Fig. 9. The determination of each mode was performed by capturing deflections of incident light from the mirror. The maximum response for the tilt mode (yellow) is shifted to a smaller frequency as $V_{offset,a}$ increases. In contrast, the tip mode (blue) increases. The increase in amplitude as the offset voltage is increased is an artifact of the constant voltage bias. A 3 mV peak-to-peak excitation corresponds to a greater power dissipation amplitude for a greater offset voltage and, consequently, a larger total energy in the system.

In contrast, if $V_{offset,b}$ is increased from 0 mV the tilt mode (yellow) is shifted to higher frequencies while the tip mode (blue) is shifted to lower frequencies. It is important to note the change in piston mode response and higher order tip/tilt modes (~ 2.6 kHz) in response to the offset variation. However, these changes are not well understood as they are difficult to distinguish at low drive amplitudes. For both offset variations, the overall mode separations are similar and are summarized in Table 1.

$V_{offset,a}$ or $V_{offset,b}$	Offset Power (mW)	Tip Mode (kHz)	Tilt Mode (kHz)	Mode Separation (Hz)
a	24	1.68	1.39	290
a	12	1.66	1.43	230
a,b	0	1.55	1.55	0
b	12	1.64	1.42	220
b	24	1.65	1.33	320

Table 1: Summary mode separation due to mechanically straining specific sets of serpentine springs.

5 CONCLUSIONS

An improvement of the static angular range compared to previous results was obtained by shortening the bimorph legs. While the total range remained consistent with previous results, the full range can be achieved without the use of differential power bias with an offset, thus reducing the required power to 25 mW. However, this produces a decrease in the vertical range to 168 μm compared to the previous 300 μm vertical range.

The functionality of the serpentine springs can be expanded beyond the mechanism for large deflections and used as a mechanical tool to alter the response frequency of the resonant modes. By adding strain to specified spring pairs, the degeneracies in the system can be lifted. Additionally, the strain can be tuned to increase the response for one of the degenerate modes while dampening the other as demonstrated in Fig. 9.

6 ACKNOWLEDGMENTS

This work was supported primarily by the Engineering Research Centers Program of the National Science Foundation under NSF Cooperative Agreement No. EEC-0812056.

REFERENCES

[1] J. Morrison, M. Imboden, T. D. C. Little, and D. J. Bishop, "Electrothermally actuated tip-tilt-piston micromirror with integrated varifocal capability," *Opt. Express*, vol. 23, no. 7, p. 9555, 2015.

[2] S. Sung, W. T. Sung, C. Kim, S. Yun, and Y. J. Lee, "On the mode-matched control of MEMS vibratory gyroscope via phase-domain analysis and design," *IEEE/ASME Trans. Mechatronics*, vol. 14, no. 4, pp. 446–455, 2009.

[3] D. Koester, A. Cowen, and R. Mahadevan, "PolyMUMPs design handbook," *MEMSCAP Inc*, 2003. [Online]. Available: http://www.memscap.com/products/mumps/polymumps/reference-material. [Accessed: 15-Dec-2014].

[4] K. Gall, M. L. Dunn, Y. Zhang, and B. a. Corff, "Thermal cycling response of layered gold/polysilicon MEMS structures," *Mech. Mater.*, vol. 36, no. 1–2, pp. 45–55, Jan. 2004.

[5] R. Bauer, G. Brown, L. Li, and D. Uttamchandani, "A novel continuously variable angular vertical comb-drive with application in scanning micromirror," *Proc. IEEE Int. Conf. Micro Electro Mech. Syst.*, pp. 528–531, 2013.

[6] J. I. Lee, P. Sunwoo, E. Youngkee, J. Bongwon, and J. Kim, "Resonant frequency tuning of torsional microscanner by mechanical restriction using MEMS actuator," *Proc. IEEE Int. Conf. Micro Electro Mech. Syst.*, pp. 164–167, 2009.